

# Numerical Analysis of Effect of Waveform Micropile on Foundation Underpinning During Building Vertical Extension Remodeling

Wang, Cheng-Can\*, Jang, Youngeun\*\*, Kim, Seok-Jung\*\*\*, Han, Jin-Tae\*\*\*\*  
왕성찬\* · 장영은\*\* · 김석중\*\*\* · 한진태\*\*\*\*

## 수치해석을 통한 수직증축 리모델링시 파형 마이크로파일의 보강효과 분석

### ABSTRACT

Micropiles are widely used for foundation underpinning to enhance bearing capacity and reduce settlement of existing foundation. In this study, the main objective is to evaluate underpinning performance of a newly developed micropile called waveform micropile for foundation underpinning during vertical extension. Finite element method (FEM) was used to evaluate the underpinning performance of waveform micropile in terms of load-settlement response of underpinned foundation and load sharing behavior. For comparison, underpinning effects of three conventional micropiles with different lengths were also discussed in this study. Numerical results of load-settlement response for single pile demonstrated that bearing capacity and axial stiffness of waveform micropiles were higher than those of conventional micropiles because of the effect of shear keys of waveform micropiles. When additional loads 20 %, which is according to design loads of the vertical extension, were applied to the underpinned foundation, load sharing capacity of waveform micropile was 40 % higher than conventional micropile at the same size. The waveform micropile also showed better underpinning performance than the conventional micropile of length 1~1.5 times of waveform micropile.

**Key words :** Vertical extension, Foundation underpinning, Micropile, Waveform micropile, Numerical analysis

### 초 록

기존건물의 수직증축시, 추가되는 증축하중을 지지하기 위해서 기초를 보강하는 것은 필수적이다. 일반적으로 기초의 지지력을 증대시키고 침하를 감소시키기 위하여 마이크로파일공법이 널리 활용되고 있다. 본 연구에서는 기존의 마이크로파일에 전단키가 추가된 새로운 형식의 파형 마이크로파일을 활용하여 연구를 수행하였다. 유한요소해석법(FEM)을 통해 기초보강시 파형마이크로파일의 하중침하거동과 하중분담율을 평가하였으며, 3가지 길이 다른 일반적인 마이크로파일들의 지지거동과 비교를 통해 보강효과를 확인하였다. 해석 결과, 파형마이크로파일의 지지력과 축강성이 일반 마이크로파일보다 크게 나타났으며, 이는 파형 마이크로파일의 전단키에 의한 효과인 것으로 판단된다. 또한, 수직증축

\* 과학기술연합대학원대학교(UST) 지반시공간공학과 박사과정 (University of Science & Technology · wangchengcan@kict.re.kr)

\*\* 울산과학기술원 도시환경공학연구부 박사후연구원 (Ulsan National Institute of Science and Technology · yeyang@unist.ac.kr)

\*\*\* 중신회원 · 한국건설기술연구원 수석연구원 (Korea Institute of Civil Engineering and Building Technology · seokjungkim@kict.re.kr)

\*\*\*\* 중신회원 · 교신저자 · 한국건설기술연구원 연구위원, UST 교수

(Corresponding Author · Korea Institute of Civil Engineering and Building Technology · jimmyhan@kict.re.kr)

Received November 20, 2018/ revised December 11, 2018/ accepted January 14, 2019

리모델링 시, 기존하중 대비 20 %의 증축하중이 재하될 때, 파형마이크로파일의 하중분담율이 동일한 길이의 일반 마이크로파일에 비해 약 40 % 증가하였으며, 보강효과는 길이 1~1.5배의 일반적인 마이크로파일보다 우수한 것으로 나타났다.

**검색어** : 수직증축, 기초보강, 마이크로파일, 파형 마이크로파일, 수치해석

## 1. Introduction

Because of rapid growth of population and limited land resources, building remodeling with vertical extension becomes an economical and effective way to enhance the utilization of existing buildings. In Korea, the government has published a statement that apartment buildings with more than 12 floors aged more than 15 years could be vertically extended up to 2-3 floors (MOLIT, 2013). In this case, foundation underpinning is essential to enhance the bearing capacity and reduce the settlement of an existing foundation in order to resist to applied loads from additional floors. Several technologies are available to underpin foundations (Thornburn and Littlejohn, 2014; Cole, 1993). Due to a limited spacing between existing piles and applicability for in-situ construction, micropile underpinning technology is widely used for existing foundation.

A micropile is a small-diameter, drilled, and grouted pile with a central steel bar. Generally, micropiles are between 100 and 300 mm in diameter, 20 m to 30 m in length, and 300 to 1000 kN in compressive or tensile service load (FHWA, 2005). The installation of micropiles causes minimal disturbance to adjacent structures, soils, and the environment. They can also be installed in restrictive conditions at any angle. The technology of micropiling was introduced by Lizzi in the early 1950s (Lizzi, 1982). Since then, it has been widely used to reinforce existing foundations in static and dynamic environments and support slopes since the 1980's (Bruce et al., 1985; Han and Ye, 2006a; Han and Ye, 2006b; Isam et al., 2012; Sadek et al., 2004; Babu et al., 2004; Esmaili et al., 2012).

In the design of underpinning for existing foundation subjected to additional loads, load sharing by existing and underpinning piles should be considered. Underpinning pile needs to share partial loads for existing piles in order to prevent exceeding existing pile's allowable load. To optimize an efficient arrangement of underpinning piles, one effective way is to improve the underpinning pile's load sharing capacity. Wang and Han(2017) has demonstrated that load sharing capacity of underpinning pile increased with its increasing stiffness by numerical analysis.

In Korea, a new type of micropile named waveform micropile was developed by Jang and Han (2014). Waveform micropile has wave-shaped grout by jet grouting method to enhance its skin resistance along the shaft of the pile. Bearing capacity and construction efficiency of waveform micropiles have been verified to be higher than those of conventional micropiles by full-scale field tests, centrifuge tests, and numerical analysis (Jang and Han, 2014; Jang and Han, 2015; Jang and Han, 2017; Jang and Han, 2018). However, the application of waveform micropile as an underpinning element has not been sufficiently investigated previously.

To enhance underpinning effect and construction efficiency of micropile during vertical extension, the main objective of this study was to evaluate underpinning effect of waveform micropile of in terms of reducing final settlement and load sharing ratio (LSR) by numerical analysis. Moreover, underpinning effects of three conventional micropiles of different lengths were also evaluated and compared to those of waveform micropiles.

## 2. Waveform Micropile

Waveform micropile is a new type of micropile with shear keys along the pile's shaft. Shear keys, which can enhance the shaft resistance in compressive stratum, are constructed by jet grouting method. Due to constructability of jet grouting method, it is applied only in the soil layers. The construction process is shown in Fig. 1. It involves the following steps: (a) drilling, (b) injection of grout to develop waveform micropile, (c) installation of steel reinforcement, and (d) Completion. This construction method of waveform micropile has been demonstrated to be more economical than that of conventional micropile (Jang and Han, 2014). Fig. 2 shows schematics of conventional micropile and waveform micropile. For case of waveform micropile, diameter of shaft part is 300 mm, and diameter of shear key part is 500 mm, which is 1.7 times larger than the diameter of the pile's shaft. Based on full-scale experimental results and centrifuge experimental results, it is demonstrated that bearing capacity of a waveform micropile

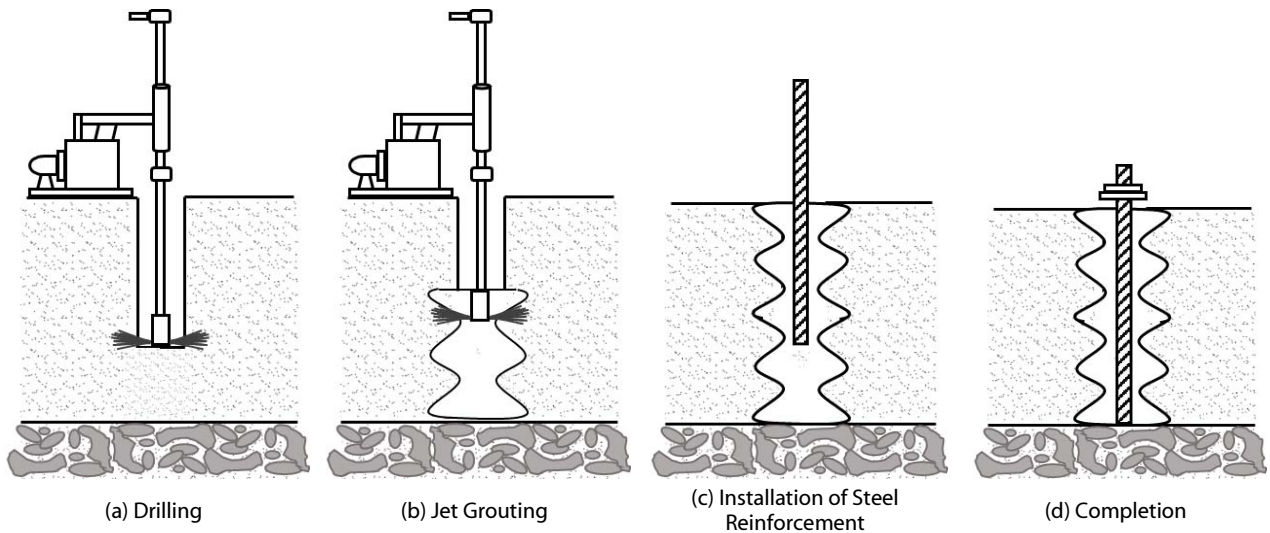


Fig. 1. Construction Method of Waveform Micropile (Jang and Han, 2017)

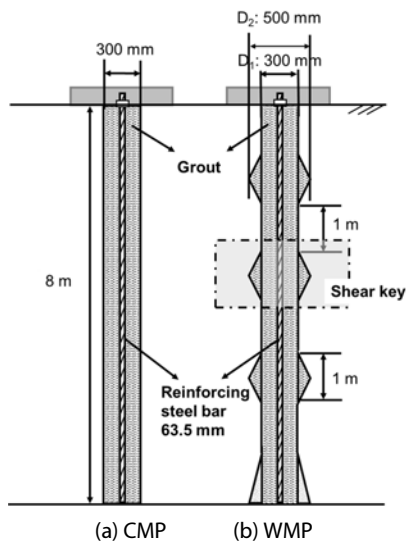


Fig. 2. Comparison of Conventional Micropile (CMP) and Waveform Micropile (WMP)

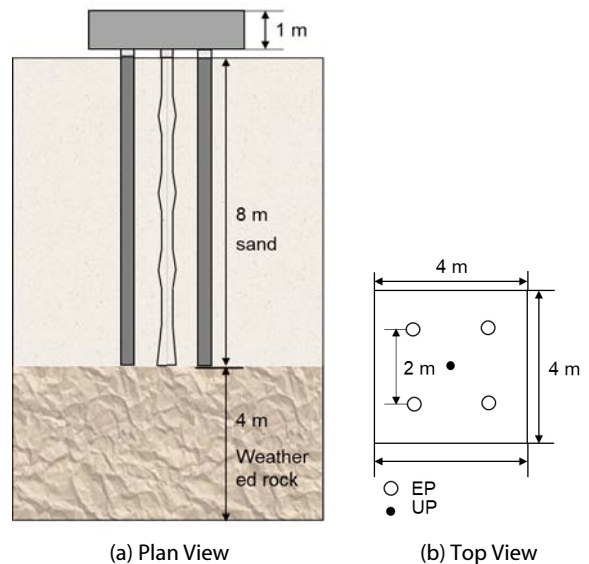


Fig. 3. Geometry of Piled Foundation

is 50 % higher than that of conventional micropile at the same size (Jang and Han, 2017; Jang and Han, 2018).

### 3. Method of Analysis

#### 3.1 Numerical Model for Pile Foundation

A 3D numerical model was developed to simulate a series of cases of foundation underpinning with finite element code PLAXIS 3D (Plaxis, 2005). Fig. 3 exhibits a schematic sketch of the numerical model developed in this investigation. The model

consisted of a 4×4×1 m raft with four existing piles (EP) and one underpinning pile (UP). General prestressed concrete piles (PCP) widely used in 1990s as foundation components were modeled as existing piles. Three conventional micropiles (CMP) with different lengths and one waveform micropile (WMP) were used as underpinning piles for comparison with the micropile’s underpinning effect. Details of the size of these piles are presented in Table 1. The mesh was extended in both horizontal direction to a width of 10 m and vertical direction to a height of 20 m. Soils are divided into layers in this analysis: 0-8 m of sand layer and

Table 1. Size of Test Pile

Test pile	Length (m)	Diameter (mm)
PCP	8	350
WMP	8	D1:300/ D2: 500
CMP1	8	300
CMP2	10	300
CMP3	12	300

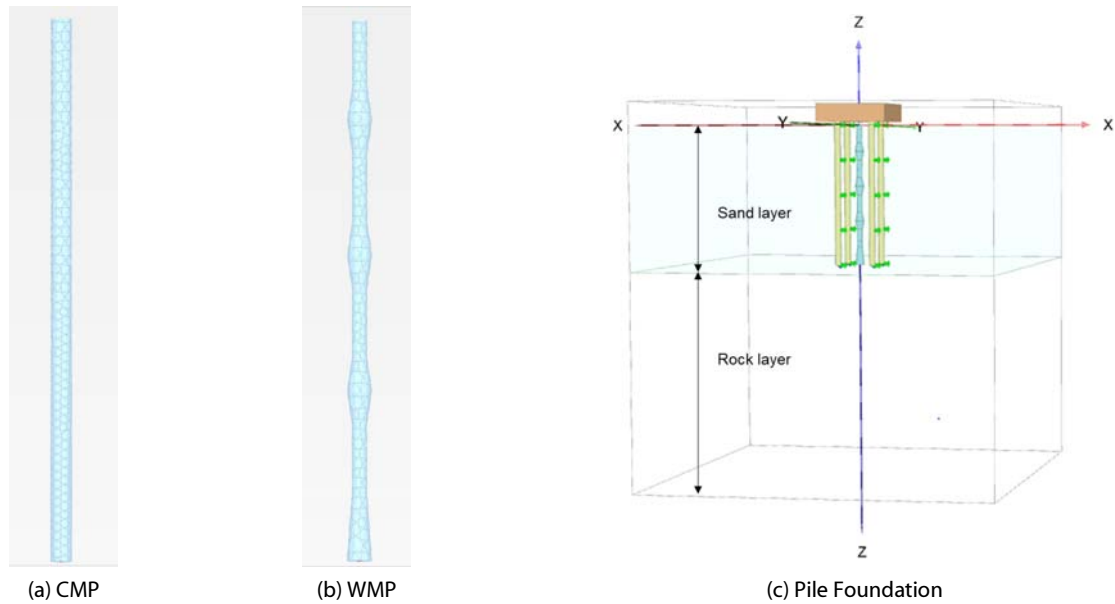


Fig. 4. Modeling of Micropile and Foundation in Plaxis

8-20 m of rock layer. Soil behavior was determined as Mohr-Coulomb model. Not considering material failure in this analysis, prestressed concrete piles and micropiles were modeled as linear-elastic model. As conventional micropiles consist of grout materials and a central steel bar, to simplify the simulation model, composite young's modulus  $E_{tot}$  combined with material of grout and steel bar was used. It is defined as follows:

$$E_{tot} = \frac{E_{grout}A_{grout} + E_{steel}A_{steel}}{A_{tot}} \quad (1)$$

Where  $E_{tot}$  is composite young's modulus of waveform micropile;  $A_{tot}$  is the area of waveform micropile;  $E_{grout}$  and  $E_{steel}$  are young's modulus of grout and steel used for waveform micropile, respectively;  $A_{grout}$  and  $A_{steel}$  is the area of grout part and steel part of waveform micropile, respectively.

For waveform micropile, due to complex configuration of the

pile, models of grout component and steel bar were built separately. Grout was modeled as linear-elastic solid model while the steel bar was modeled as beam elements. Fig. 4 shows the geometry of an example of a conventional micropile and a waveform micropile in numerical analyses. Material properties of soils and piles used in these analyses are shown in Tables 2 and 3. They were taken from Wang et al. (Wang et al., 2017; Wang et al., 2018a; Wang et al., 2018b). The soil-pile interface was described by  $R_{inter}$ , the interface strength reduction factor (Plaxis, 2005).  $R_{inter}$  was defined as:

$$c_i = R_{inter}c_{soil} \quad (2)$$

$$\tan\phi_i = R_{inter}\tan\phi_{soil} \quad (3)$$

Where  $c_i$  and  $\phi_i$  are cohesion and frictional angles of the interface;  $c_{soil}$  and  $\phi_{soil}$  are cohesion and frictional angles of the soil;  $R_{inter} = 0.67$ , a representative value in Plaxis 3D.

**Table 2. Properties of Piles**

Description	EP	UP				Raft
	PCP	CMP		WMP		
Material	Concrete	Grout	Steel	Grout	Steel	Concrete
Diameter (mm)	350	300	63.5	D1: 300 D2: 500	63.5	4 X 4
Unit Weight (kN/ m <sup>3</sup> )	23.5	23.5	78.5	23.5	78.5	23.5
Young's Modulus (GPa)	24	32.3		24	210	24
Material Model	Linear Elastic				Beam	Linear Elastic

**Table 3. Properties of Soils**

Description	Sand	Weathered Rock
Depth (m)	0-8	8-20
Unit Weight (kN/ m <sup>3</sup> )	19	21
Material Model	MC	MC
Interface strength factor, R <sub>inter</sub>	0.67	0.67
Frictional Angle, $\phi$ (°)	34	39
Cohesion, c (kN/ m <sup>2</sup> )	10	30
Dilatancy Angle, $\psi$ (°)	4	9
Young's Modulus, E (KPa)	3.5E4	3.0E5
Poisson Ratio, $\nu$	0.3	0.28

## 4. Results and Discussion

### 4.1 Single Pile Tests

Fig. 5 presents the load-settlement behavior of five single piles under compression. The curve clearly shows that the WMP has higher load capacity than conventional micropiles. Because of no significant failure point shown in the curve, the ultimate bearing capacity of each pile was estimated corresponding to pile head settlement of 25.4 mm (Terzaghi and Peck, 1967; Touma and Reese, 1974). Failure mechanism is considered to be developed only in the soil due to the assumption that no failure occurred in the pile material. A factor safety of 3 was applied to calculate the allowable bearing capacity of single piles. Table 4 summarizes the proposed allowable bearing capacities of PCP, CMP1, CMP2, CMP3, and WMP (567 kN, 328 kN, 400 kN, 483kN, 877 kN), respectively. Shear keys along the pile's shaft enhanced shaft resistance in both compressive stratum and bearing stratum compared to conventional micropiles for which the shaft resistance was mainly mobilized in the bearing stratum. Bearing capacity of waveform micropile was 1.5 times more compared to prestressed concrete pile and 2 ~ 4 times more compared to

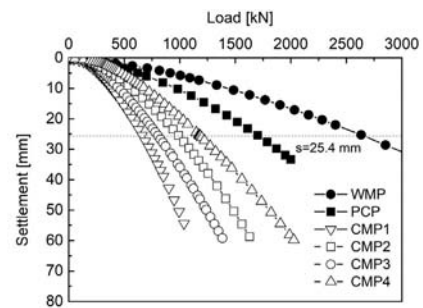


**Fig. 5. Load Settlement Response of Single Piles**

**Table 4. Summary of Bearing Capacity of Single Piles**

Type		Q <sub>ult</sub> (kN)	Q <sub>all</sub> (kN)
UP	CMP1	985	328
	CMP2	1200	400
	CMP3	1450	483
	WMP	2630	877
EP	PCP	1700	567

conventional micropiles depending on pile's length. Trends of numerical results in the present study are in agreement with those reported by Jang and Han (2018).

### 4.2 Axial Stiffness of piles

Axial stiffness  $k_v$  of a pile is defined as the slope of load-settlement curve. It can be obtained from single pile loading test under compression based on properties of the pile and soils (Randolph, 1994) or empirical equation based on numerous field data (KHS, 2008; Koichi et al., 1996). The empirical equation proposed by Korea Highway Bridge Design Standard (2008) is shown below:

$$k_v = \alpha \frac{A_p E_p}{L} \tag{4}$$

Where  $k_v$  is axial stiffness of a pile (kN/m);  $A_p$ ,  $E_p$ , and  $L$  are pile’s area (m<sup>2</sup>), Young’s modulus (KPa), and length (m), respectively.

$\alpha$  is stiffness factor depending on the type and construction method of piles as follows:

$$\text{Driven pile} : \alpha = 0.014 \left( \frac{L}{D} \right) + 0.72 \tag{5}$$

$$\text{Vibration pile} : \alpha = 0.017 \left( \frac{L}{D} \right) - 0.014 \tag{6}$$

$$\text{Cast in situ pile} : \alpha = 0.031 \left( \frac{L}{D} \right) - 0.15 \tag{7}$$

$$\text{Bored pile} : \alpha = 0.010 \left( \frac{L}{D} \right) + 0.36 \tag{8}$$

In this study, prestressed concrete pile (PCP) used as existing pile is a kind of precast driven pile. Eq. (4) was used to calculate PCP’s axial stiffness. Micropile used as underpinning pile is a kind of cast in situ pile. The value of Young’s modulus and area

of each pile for calculation is in accordance to the data used in numerical analysis shown in Table 2. Eq. (7) was applied to calculate MP’s axial stiffness. Piles’ axial stiffness estimated by Eq. (5),  $k_{vs}$ , and estimated by slope of load-settlement curve based on Fig. 5,  $k_{ve}$ , are calculated in Table 5. It is seen that  $k_{vs}$  obtained in the loading test is good agreement with that proposed by KHS for WMP and PCP. However, for comparison of conventional micropiles, the value of  $k_{vs}$  showed that stiffness of conventional micropile is significantly affected by its socket length, but it is not considered in Eq.(4).

### 4.3 Construction Procedure of Vertical Extension of an Existing Building

Superstructure of a building includes frame structure and finishing materials. Loads of frame structure occup about 60 % of the total superstructural loads in the design (KICT, 2013). Before doing the construction of vertical extension of an existing building, all the materials expect frame structures should be removed. The construction procedure of an existing building remodeled with vertical extension is shown as following steps: 1) removing the finishing material; 2) drilling holes and installing underpinning piles; 3) applying additional floors; and 4) recovering the finishing materials. In this analysis, the simulation process considering procedure of vertical extension construction was described as: 1) loading step (construction of an existing building); 2) unloading step (removal of finishing material loads); 3) installation of a micropile; and 4) reloading step (vertical extension). In the loading stage, the applied load was determined to be 1500 kN based on allowable bearing capacity of the existing pile. After installation of existing foundations, a load of 1500 kN (100 %) was applied to the foundation for simulation of the existing building. In the unloading stage, 40 % of the load (600 kN) was

Table 5. Summary of Stiffness of Single Piles

Type		$k_{vs}$ *(kN/m)	$k_{ve}$ **(kN/m)	K***
UP	WMP	194761	193116	1.28
	CMP1	146126	193116	0.96
	CMP2	154140	201678	1.01
	CMP3	209800	207386	1.38
EP	PCP	152000	169881	-

\* $k_{ve}$  : axial stiffness of a pile which is calculated by Eq. (4).

\*\* $k_{vs}$  : axial stiffness of a pile which is estimated by initial slope of load-settlement curve.

\*\*\* K is the stiffness ratio of underpinning pile to existing pile based on  $k_{vs}$ .

removed. A micropile was then installed to underpin the existing foundation. At the reloading stage, a load from 1500 kN to 2250 kN was applied in an increment of 150 kN as a vertical extension process.

#### 4.4 Load Settlement Response of Underpinned Foundation

The load settlement curve for existing foundation under loading, unloading, underpinning, and reloading is plotted in Fig. 6. A simulation of loading test of a raft with four PC piles without underpinning was also built to establish a reference point to evaluate the behavior of foundation underpinning with a micropile.

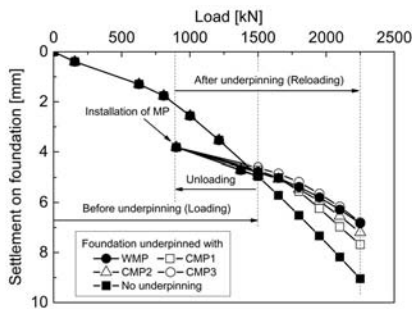


Fig. 6. Load Settlement Behavior of Underpinned Foundation with Different Micropiles

The final settlement of existing foundation without underpinning under a load of 2,250 kN was 9.1 mm. For cases of foundation underpinning with micropiles, after installation of a micropile, load settlement response showed stiffer behavior compared to foundation without underpinning during the reloading stage. The underpinning micropile reduced the final settlement of existing foundation. Fig. 6 shows that the settlement of underpinned foundation decreases with an increase in socket length of conventional micropile. This is because the frictional resistance of a micropile is mainly developed along the pile’s shaft in the bearing stratum. Moreover, when WMP and CMP1 at the same length were compared, the foundation underpinned with WMP showed much stiffer behavior than that with CMP1. The final settlement of foundation underpinned with WMP was reduced about 10 % than that with CMP1. When WMP and CMP3 were compared, although the length of CMP3 was 1.5 times that of WMP, final settlement was almost the same for the two. This implies that waveform micropile with shear keys has better performance in reducing final settlement than a conventional micropile with the same size. Moreover, to have the same performance, underpinning with WMP can decrease length 30 % than that with conventional micropile, thus decreasing construction and material cost.

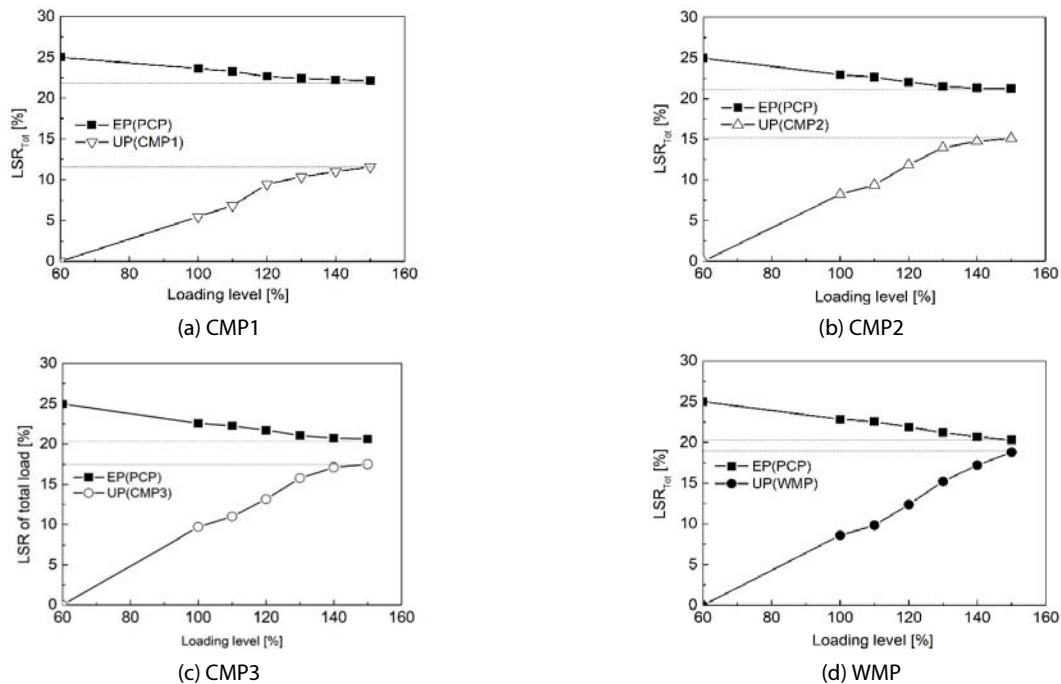


Fig. 7. Total Load Sharing Ratio of Existing and Underpinning Pile

### 4.5 Load Sharing Behavior of Underpinned Foundation Considering Loading Stages

Load sharing ratio (LSR) was used to describe the percentage of carried load of a pile divided by the applied load to the foundation. The definition of LSR for a pile is shown below:

$$LSR_{Tot} = \frac{\text{Carried load of each pile}}{\text{Total applied load}} \tag{9}$$

$$LSR_{Add} = \frac{\text{Carried load of each pile}}{\text{Additional applied load}} \tag{10}$$

The carried load of a pile was measured on the head of the pile. Fig. 7 illustrates influence of micropile’s length and shape on load sharing capacity of underpinning pile of total applied load. During loading and unloading, applied loads were carried by existing piles only. Each PCP carried 25 % of the total load. After installation of a micropile and reloading to the underpinned foundation, the micropile began to carry partial loads. The load sharing capacity increased with increase of applied load while LSR of PCP gradually decreased from 25 %. As shown in Fig. 7, LSRs of WMP and CMP3 with high stiffness increased sharply with applied loads. On the contrary, LSRs of CMP1 and CMP2 increased slowly with applied loads and gradually converged. After loading was completed, the LDR of WMP was the highest, followed by that of CMP3, CMP2, and CMP1. It also can be seen load sharing capacity of underpinning is increased with increasing socket length.

Fig. 8 exhibits load sharing of additional applied load of each micropile during reloading stage. It was noted that additional loads were shared by exiting and underpinning piles together. For conventional micropiles, load sharing ratio increased with

applied additional loads and gradually converged. At the final loading level, LSRs of CMP1, CMP2, and CMP3 were 20 %, 25 %, and 29 %, respectively. However, load sharing of WMP kept increasing, reaching 31 % at the final loading level. If the axial stiffness of existing pile is the same as that of the underpinning piles, each pile would share 20 % of load in ideal circumstance. However, CMP1 carried almost 20 % load as shown in Fig. 8 while axial stiffness ratio K of CMP1 to existing pile was less than 1 as shown in Table 5. This phenomenon was also observed in other cases. It can be explained that the axial stiffness of a pile is varied with applied loads. It is decreased with increasing loading due to the non-linear behavior of soil-pile interaction. Compared to the initial slope of load-settlement curve, at the stage of installation of underpinning pile, the real axial stiffness of the existing pile is lower. Thus, the relationship between load sharing and stiffness of underpinning and existing piles is a key in design of foundation underpinning.

To better understand the effect of a pile’s axial stiffness on load sharing behavior, the relation of normalized load sharing ratio  $\lambda$  to normalized stiffness K of underpinning pile to existing pile is summarized in Fig. 9. 2 distinct parts were divided in the curve. For underpinning with conventional micropile, if stiffness of underpinning is lower than existing pile, load sharing capacity of underpinning pile is not significant. If stiffness of underpinning pile is higher than existing pile, which K is more than 1,  $\lambda$  increases as a slope 0.5 with increase of stiffness ratio K. Moreover, load sharing capacity of underpinning pile increased with increasing of applied loads. In the practical project of vertical extension of existing apartment buildings, because of the statement mentioned in the introduction, 20 % of additional load can be applied on the existing building. At reloading level of 120 %

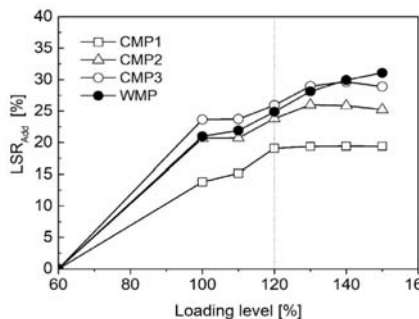


Fig. 8. Comparison of Additional Load Sharing Ratio by Underpinning Piles

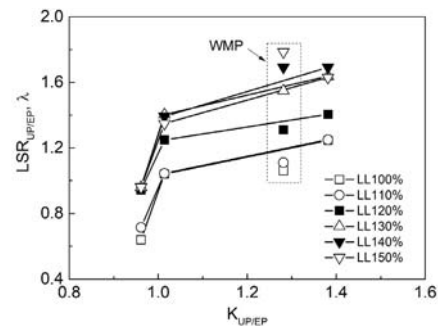


Fig. 9. Normalized Load Sharing vs. Normalized Stiffness of Underpinning Pile to Existing Pile



shown in Fig. 9, assuming all piles are installed perfectly and no effect on the constructability in situ, it is seen that load sharing of underpinning pile to existing pile varies from 1.0 to 1.4 with increasing stiffness ratio from 1 to 1.4. In addition, load sharing capacity of waveform micropile is more remarkable at high loading level. These results are useful for providing a proper underpinning method considering pile's axial stiffness for practical vertical extension work.

$$\lambda = \frac{LSR_{addUP}}{LSR_{addEP}} \quad (11)$$

$$K = \frac{k_{vsUP}}{k_{vsEP}} \quad (12)$$

## 5. Conclusions

In this study, FEM numerical analysis was carried out to investigate waveform micropile's underpinning effect during building remodeling with vertical extension. Results were compared to those of foundation underpinning by conventional micropiles with different lengths.

- (1) Bearing capacity and axial stiffness of a pile were firstly estimated by single pile loading test. Waveform micropile showed stiffer behavior and higher bearing capacity than conventional micropile with the same diameter and length. It had similar behavior to a conventional micropile with longer length with 1.5 times of waveform micropile length.
- (2) Results of numerical analysis demonstrated that underpinning with micropile could reduce the total settlement of foundation and carry partial loads from existing piles. The underpinning performance of conventional micropile increased with increasing socket length of a pile. This is because socket length plays an important role in increasing axial stiffness of a pile.
- (3) When waveform micropile and conventional micropile with the same length were compared, total settlement and load sharing in case of foundation underpinned with waveform micropile were 10 % less and 40% higher than those with conventional micropile under design loads of the vertical extension, which the additional load is 20 %. Waveform micropile had similar underpinning performance to conventional

micropile with longer socket length with 1.5 times of waveform micropile length. These results imply that, in practical construction, waveform micropile would be a more economical and effective method for foundation underpinning than conventional micropile to save construction and material cost.

- (4) The ratio of load sharing by underpinning pile to existing pile increased linearly with increasing stiffness ratio  $K$  of underpinning pile to existing pile if underpinning pile is stiffer than existing pile. This finding is useful for providing a proper underpinning method considering pile's axial stiffness for vertical extension work.

In addition, as the limited numerical results in this study, field tests or centrifuge model tests will be carried out in order to obtain more accurate results.

## Acknowledgements

This research was supported by a grant from "Development of Technologies for Structural safety on Vertical Extension for Existing Apartment Buildings" which is funded by the Korea Agency for Infrastructure Technology Advancement.

An earlier version of this paper was presented at KSCE 2018 CONVENTION and was published in this Proceedings.

## References

- Babu, G. S., Murthy, B. S., Murthy, D. S. N. and Nataraj, M. S. (2004). "Bearing capacity improvement using micropiles: a case study." *GeoSupport 2004: Drilled Shafts, Micropiling, Deep Mixing, Remedial Methods, and Specialty Foundation Systems*, pp. 692-699.
- Bruce, D. A., Ingle, J. L. and Jones MR. (1985). "Recent Examples of Underpinning Using Minipiles." *2nd Int. Conf. on Structural Faults and Repairs*, London, pp. 13-28.
- Cole, K. W. (1993). "Conventional piles in underpinning." *In underpinning and Retention*, Springer US, pp. 63-83.
- Esmaili, M., Nik, M. G. and Khayyer, F. (2012). "Experimental and numerical study of micropiles to reinforce high railway embankment." *International Journal of Geomechanics*, Vol. 13, pp. 729-744.
- Federal Highway Administration (FHWA) (2005). *Micropile Design and Construction: Reference Manual*, Federal Highway Administration (FHWA) U.S. Department of Transportation, Washington, D.C. Publication No. FHWA- NHI-05-039.

- Han, J. and Ye, S. L. (2006a). "A field study on the behavior of micropiles in clay under compression or tension." *Canadian Geotechnical Journal*, Vol. 43, No. 1, pp. 19-29.
- Han, J. and Ye, S. L. (2006b). "A field study on the behavior of a foundation underpinned by micropiles." *Canadian Geotechnical Journal*, Vol. 43, pp. 30-42.
- Isam, S., Hassan, A. and Mhamed, S. (2012). "3D elastoplastic analysis of the seismic performance of inclined micropiles." *Computers and Geotechnics*, Vol. 39, pp. 1-7.
- Jang, Y. E. and Han, J. T. (2014). "Development on the micropile for applying to artificial ground above railroad site." *Advanced Science and Technology Letter*, Vol. 55, pp. 43-46.
- Jang, Y. E. and Han, J. T. (2015). "Study of load capacity of waveform micropile by centrifuge test." *The Twenty-fifth (2015) International Ocean and Polar Engineering Conference*, pp. 700-706.
- Jang, Y. E. and Han, J. T. (2017). "Field study on axial bearing capacity and load transfer characteristic of waveform micropile." *Canadian Geotechnical Journal*, Vol. 55, No. 5, pp. 653-665.
- Jang, Y. E. and Han, J. T. (2018). "Analysis of the shape effect on the axial performance of a waveform micropile by centrifuge model test." *Acta Geotechnica*, pp. 1-14.
- KHS (2008). Korea Highway Bridge Design Standard, Explanation, pp. 885-887 (in Korean).
- Korea Institute of Civil Engineering and Building Technology (KICT) (2013). Development of Pre-loading Method for Reinforcement Piles of Apartment Remodeling (1). KICT2013-260, 23-61 (in Korean).
- Koichi, O., Hiroshi, K. and Motofumi, S. (1996). "Up-down vibration effects on bridge piers." *Japanese Geotechnical Society*, Vol. 36, pp. 211-218.
- Lizzi, F. (1982). The pali radice (root piles). "Symposium on soil and rock improvement techniques including geotextiles." *Reinforced Earth and Modern Piling Methods*, Bangkok, Paper D-3.
- Ministry of Land, Infrastructure and Transport (MOLIT) (2013). Housing Act, Korea Ministry of Land, Infrastructure and Transport, p. 2.
- Plaxis, B. V. (2005). PLAXIS User's manual.
- Randolph, M. (1994). "Design methods for pile groups and piled rafts." *Pro. of 13<sup>th</sup> ICSMFE*, New Delhi, India, Vol. 5, pp. 61-82.
- Sadek, M. and Isam, S. (2004). "Three-dimensional finite element analysis of the seismic behavior of inclined micropiles." *Soil Dynamics and Earthquake Engineering*, Vol. 24, pp. 473-485.
- Terzaghi, K. and Peck, R. B. (1967). *Soil Mechanics in Engineering Practice*, 2<sup>nd</sup> ed, John Wiley and Sons, New York.
- Thorburn, S. and Littlejohn, G. S. (2014). *Underpinning and Retention*, CRC Press.
- Touma, F. T. and Reese, L. C. (1974). "Behavior of bored piles in sand." *Journal Geotechnical Engineering Division, ASCE*, Vol. 100, No. 7, pp. 749-761.
- Wang, C. C. and Han, J. T. (2017). "3D FEM analysis on load distribution behavior for pile foundation during vertical extension of apartment building." *Pro. of 19<sup>th</sup> Int. Conf. on Soil Mechanics and Geotechnical Engineering*, pp. 1929-1934.
- Wang, C. C., Han, J. T., Jang, Y. E., Ha, I. S. and Kim, S. J. (2018a). "Study on the effectiveness of preloading method on reinforcement of the pile foundation by 3D FEM analysis." *Journal of the Korean Geotechnical Society*, Vol. 34, No. 1, pp. 47-57 (in Korean).
- Wang, C., Jang, Y., Kim, S. and Han, J. T. (2018b). "Effect of waveform micropile on foundation underpinning during building remodeling with vertical extension." *GeoChina 2018*, pp. 120-130.